Detection of Microwave Spin Pumping Using the Inverse Spin Hall Effect

C. Hahn, G. de Loubens, M. Viret, and O. Klein*
Service de Physique de l'État Condensé (CNRS URA 2464), CEA Saclay, 91191 Gif-sur-Yvette, France

V. V. Naletov
Service de Physique de l'État Condensé (CNRS URA 2464), CEA Saclay, 91191 Gif-sur-Yvette, France
Institute of Physics, Kazan Federal University, Kazan 420008, Russian Federation

J. Ben Youssef
Université de Bretagne Occidentale, Laboratoire de Magnétisme de Bretagne CNRS, 6 Avenue Le Gorgeu, 29285 Brest, France
(Received 15 August 2013; published 21 November 2013)

We report on the electrical detection of the dynamical part of the spin-pumping current emitted during ferromagnetic resonance using inverse spin Hall effect methods. The experiment is performed on a YIG|Pt bilayer. The choice of yttrium iron garnet (YIG), a magnetic insulator, ensures that no charge current flows between the two layers and only the pure spin current produced by the magnetization dynamics is transferred into the adjacent strong spin-orbit Pt layer via spin pumping. To avoid measuring the parasitic eddy currents induced at the frequency of the microwave source, a resonance at half the frequency is induced using parametric excitation in the parallel geometry. Triggering this nonlinear effect allows us to directly detect on a spectrum analyzer the microwave component of the inverse spin Hall effect voltage. Signals as large as 30 μV are measured for precession angles of a couple of degrees. This direct detection provides a novel efficient means to study magnetization dynamics on a very wide frequency range with great sensitivity.

DOI: 10.1103/PhysRevLett.111.217204 PACS numbers: 85.75.−d, 76.50.+g

One great expectation of spintronics regarding information technology is the promise that pure spin currents can be generated and manipulated without their charge current counterparts [1]. Pure spin currents correspond to the transport of angular momentum in a very wide range of materials, including metals and insulators with or without magnetic order. In ferromagnetic metals, charge currents are intrinsically associated with spin currents because electrons at the Fermi level are spin polarized. Using these as injection electrodes, pure spin currents can be generated into a nonmagnetic metal in a nonlocal geometry where charges are evacuated through one electrode whereas spin diffusion can be collected by another nearby electrode [2,3]. This lateral geometry is well suited to nanostructures, but it is limited by the required current densities and the short spin diffusion lengths [4]. Another option relies on using the spin Hall effect, a phenomenon based on the spin-orbit interaction of a charge current which generates a transverse spin current in a conductor [5,6]. Pure spin currents can also be generated in ferromagnetic insulators by the spin-pumping mechanism [7–9] during magnetization precession. This effect is produced by the damping of spin waves which transfer angular momentum across an interface to a neighboring layer. The emitted pure spin current can be detected electronically in an adjacent layer by the inverse spin Hall effect (ISHE) technique using metals with strong spin-orbit coupling like Pt [10–14]. The novelty here offered by electrical detection of the spin pumping using the ISHE is that it can also be used on nonmetallic ferromagnets, including yttrium iron garnet (YIG) [9,15–22], a magnetic insulator which has unsurpassed small damping in ferromagnetic resonance (FMR). But, so far, only the dc component of the ISHE voltage induced by FMR has been measured, which is a second order effect in the precession angle. Here, we report on a direct measurement of its first order ac counterpart.

The experiments of the present study are performed at room temperature on a YIG|Pt bilayer where the YIG is a 200 nm thick epitaxial film grown by liquid phase epitaxy. A 6 nm thick Pt layer is then sputtered on top, and two contact electrodes are defined at each end. The sample is mounted on a stripline antenna generating a microwave field h oscillating at a frequency f_p as sketched in Fig. 1. At resonance of the uniform mode, the YIG emits, perpendicularly to the YIG|Pt interface, a flow of angular momentum generated by the spin-pumping effect

$$\boldsymbol{J}_s = \left(\frac{\hbar}{2eM_s}\right)^2 G_{\uparrow\downarrow}\left[\boldsymbol{M}\times\frac{\partial \boldsymbol{M}}{\partial t}\right]. \quad (1)$$

In this expression, $\boldsymbol{M}$ is the magnetization vector, whose norm is M_s, $\hbar$ is the reduced Planck constant, e the electron charge, and $G_{\uparrow\downarrow}$ the spin mixing conductance at the YIG|Pt interface in units of $\Omega^{-1}\,\mathrm{m}^{-2}$. The spin current pumped into the adjacent Pt is then converted into a charge current by ISHE

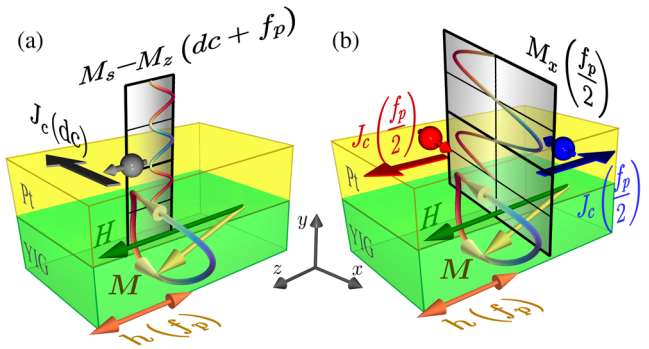

FIG. 1 (color online). Schematic representation showing the direction of the (a) dc and (b) ac charge currents produced when a pure spin current is pumped from the insulating magnetic YIG (green regions) into the strong spin-orbit Pt metal (yellow regions). The instantaneous magnetization $\boldsymbol{M}(t)$ is shown in a bivariate color map: the blue-red colors code the x component, and the gray shades code the z component. The precession of $\boldsymbol{M}$ at $f_p/2$ around $\boldsymbol{z}$ is driven by parametric excitation: it requires the pumping field h, oscillating at f_p, to be parallel to the bias magnetic field H, and the precession of (M_x, M_y) to be elliptic (thus, $M_x^2 + M_y^2$ is not a constant of the motion). The flow charts on top illustrate that $M_z = \sqrt{M_s^2 - M_x^2 - M_y^2}$ then oscillates 2 times faster than M_x or M_y. Spin-pumping currents are flowing from YIG to Pt (i.e., along the y axis). The injected angular momentum in Pt is carried by the spins (arrows attached to the electrons opposite to their angular momentum). The direction of the instantaneous charge current (flat arrow) is given by the right-hand rule; see Eq. (2).

$$\boldsymbol{J}_c = \frac{2e}{\hbar}\Theta_{\mathrm{SH}}[\boldsymbol{y} \times \boldsymbol{J}_s], \tag{2}$$

where Θ_{SH} is the spin Hall angle in Pt and $\boldsymbol{y}$ is the unit vector perpendicular to the interface (see Fig. 1).

Importantly, the flow $\boldsymbol{J}_s$ (and hence $\boldsymbol{J}_c$) has both dc and ac components [23]. The dc part of this signal is normally detected as a voltage, proportional to $\boldsymbol{J}_c(\mathrm{dc})$, that is maximum in a transverse geometry [i.e., $\perp H$; see Fig. 1(a)]. In contrast, $\boldsymbol{J}_c(\mathrm{ac})$ is maximum in a parallel geometry [i.e., $\parallel H$; see Fig. 1(b)]. It is interesting to note that for circular precession, the dc signal is second order in the precession angle θ ($\propto \sin^2\theta$, maximal for $\theta = 90°$), while its ac counterpart is first order ($\propto \sin\theta\cos\theta$ and maximal for $\theta = 45°$). Thus, the ratio of ac to dc scales as $1/\tan\theta$, which is large for small precession angles. However, the ac component is much harder to detect, as it oscillates obviously at the same frequency as that of the microwave generator producing the FMR. This microwave excitation field h induces eddy currents in any closed circuit containing the sample. These spurious ac currents are generally rather large and dominate any other contribution at the same frequency. Therefore, a clear detection of the ac spin currents has not yet been successful, as one has to carefully eliminate the large amplitude eddy currents. In this Letter, we report on the unambiguous detection of these ac spin currents emitted at ferromagnetic resonance using a specially designed system leading to an ac signal totally unpolluted by any other contribution. The key strategy here is to generate the FMR at half the frequency of the excitation source. This phenomenon is known as parametric excitation [24]. It exploits the fact that due to the ellipticity of the in-plane precession, the magnetization follows a clamshell trajectory. During a full revolution of $\boldsymbol{M}$ around its precession axis z, the z component of the magnetization M_z oscillates 2 times faster; see Fig. 1(a). This is also illustrated in Fig. 1(b) using red and blue colors to code its x component M_x. Therefore, by exciting parallel to $\boldsymbol{M}$, one can trigger the precession at half the source frequency. One should note, however, that this parallel parametric excitation is only possible in systems with low damping, since the excitation power needs to exceed a minimum threshold corresponding to a fraction of linewidth (typically below 1 Oe for YIG [24]) in order to drive the magnetization into oscillation.

Experimentally, since the technique depends sensitively on the respective orientations of the microwave excitation and the bias field, we shall measure the ratio of the dc and ac components of $\boldsymbol{J}_c$ by rotating H, the static bias magnetic field, in the film plane. For all practical purposes, the YIG slab can be considered as an infinite film, whose resonance conditions are independent of the orientation of H.

In order to characterize our sample, and in particular the electrical conversion of the pumped spin current at the YIG|Pt interface, we first perform standard FMR resonance, where the small microwave field h is perpendicular to H ($\phi_H = 90°$). It is indeed the most efficient configuration to excite the magnetization dynamics: in the case displayed in Fig. 2, the angle of precession induced in YIG at resonance by a microwave field $h = 36$ m Oe ($P = -5$ dBm) is $\theta = 1.1°$ (see the Supplemental Material [25]). The FMR signal is detected simultaneously by probing the power transmitted through the microwave line using a diode [Fig. 2(a)] and by measuring the dc ISHE voltage transversally to the static magnetization [Fig. 2(b)]. Both measurements yield the same evolution of the resonance field versus frequency following the Kittel law for an in-plane magnetized thin film; see Fig. 3(a). By measuring the diode signal at low power ($P = -20$ dBm, corresponding to $h = 6$ mOe), one can also determine in the linear regime the dependence of the linewidth on frequency, which is reported in the inset of Fig. 2(a). A linear fit yields the Gilbert damping $\alpha_G = (1.4 \pm 0.1) \times 10^{-4}$, highlighting the very small magnetic relaxation of our YIG film [22]. The inhomogeneous part to the linewidth $\Delta H_0 = 1.7 \pm 0.2$ Oe reflects sample imperfections specific to the growth process of this batch. We find that this contribution dominates the broadening below 10 GHz. The amplitude of $V_{\mathrm{ISHE}}(\mathrm{dc})$ measured at resonance allows us to determine the transport parameters at play in the electrical conversion of the pumped spin current (see the

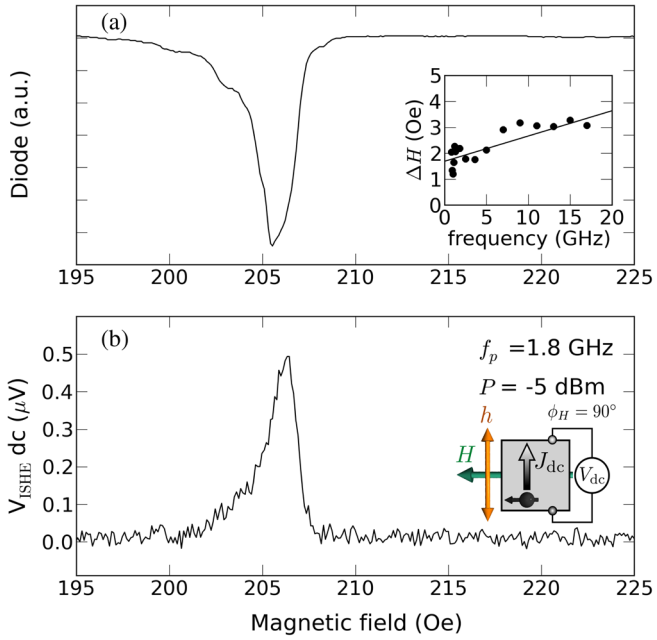

FIG. 2 (color online). Standard FMR detected using dc ISHE voltage. The pumping field h oscillating at $f_p = 1.8$ GHz is oriented perpendicularly to the static magnetic field H. (a) Larmor absorption peak of the uniform mode detected with a diode (the inset shows the dependence of the linewidth on frequency). (b) Corresponding dc ISHE voltage measured perpendicularly to H (the inset shows the geometry of the experiment).

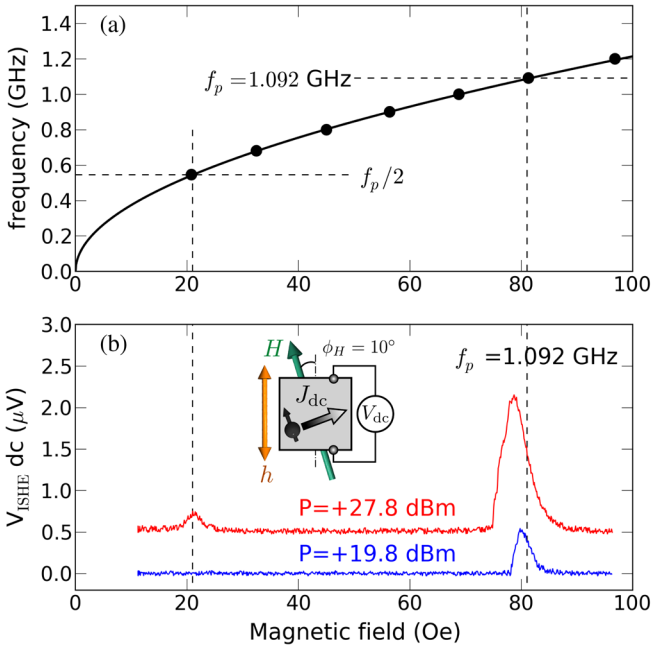

FIG. 3 (color online). Parametric excitation detected using the dc ISHE voltage. (a) Measured variation of the resonance frequency f_{res} as a function of the applied field (dots) using the standard FMR geometry (Fig. 2). The solid line is the Kittel law $f_{res} = (\gamma/2\pi)\sqrt{H(H + 4\pi M_s)}$ with $\gamma = 1.785 \times 10^7$ rad s^{-1} Oe^{-1} and $M_s = 139$ emu cm^{-3}. (b) Spin-wave mode spectra detected using the dc ISHE voltage for two different power levels. The bias field H is oriented at 10° from the pumping field h oscillating at $f_p = 1.092$ GHz (the inset shows the geometry of the experiment). At lower power (+19.8 dBm), the only peak detected in the spectrum occurs when the Larmor condition is met at f_p. At higher power (+27.8 dBm), a new peak appears in the spectrum at $f_p/2$, corresponding to the parametrically excited resonance.

Supplemental Material [25]). We find that our dc ISHE data can be well explained using typical parameters of the YIG|Pt system [21,22]: spin diffusion length $\lambda_{SD} = 2$ nm, spin Hall angle $\Theta_{SH} = 0.05$, and spin mixing conductance $G_{\uparrow\downarrow} = 10^{14}\ \Omega^{-1}\,\mathrm{m}^{-2}$.

We now wish to excite parametrically the YIG magnetization at half the applied microwave frequency $f_p/2$ by taking advantage of the clamshell shape of the precession trajectory, which is sketched in Fig. 1. For this, the component of the microwave field h parallel to the bias field H should reach the excitation threshold for parallel parametric excitation [24]. To demonstrate this effect in our sample through dc ISHE voltage measurements, we set a finite angle $\phi_H = 10°$ between h and H [see the inset of Fig. 3(b)]. Compared to the previous perpendicular geometry, the resonance condition at f_p has not changed, only the microwave field is less efficient to bring the magnetization out of equilibrium; thus, a stronger excitation power should be used to reach the same precession angle. We move momentarily to lower frequency in order to insert in the microwave circuit an additional amplifier limited in bandwidth to 1.1 GHz (see the Supplemental Material [25]). At $f_p = 1.092$ GHz and $P = +19.8$ dBm, we observe only one resonance peak at $H = 80$ Oe in Fig. 3(b). The new feature here is that if we increase the power to $P = +27.8$ dBm, a second peak appears in the spectrum at $H = 20$ Oe. Looking at the Kittel law of Fig. 3(a), we find that it corresponds to the uniform mode resonating at $f_p/2$, which is thus parametrically excited [17,18,26,27]. Thanks to the quantitative analysis of V_{ISHE}(dc) using the transport parameters determined previously, it is possible to quantify the angle of precession corresponding to this parametric excitation: $\theta = 5.1°$ (see the Supplemental Material [25]).

The next step is to directly detect the ac ISHE voltage generated at $f_p/2$ by the parametrically excited magnetization dynamics. For this, we now align the microwave field h with the bias field H ($\phi_H = 0°$) and excite the system at $f_p = 3.6$ GHz and high power $P = +24$ dBm. The two voltage leads which contact the Pt layer are connected directly into a spectrum analyzer (SA) without any preamplification scheme. By sweeping the frequency of the SA at fixed $H = 205$ Oe, we detect a large signal of amplitude 30 μV at exactly $f_p/2 = 1.8$ GHz, as can be seen in Fig. 4(a). We claim this signal to be the ac component of the pure spin current pumped from the YIG

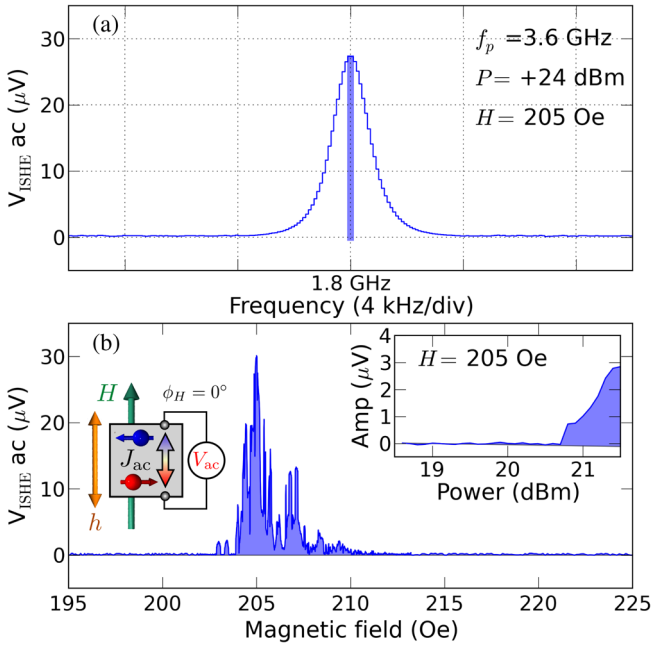

FIG. 4 (color online). Parametric excitation detected using the ac ISHE voltage. The large power (+24 dBm) pumping field h at $f_p = 3.6$ GHz is oriented parallel to the static magnetic field H. (a) The ac ISHE voltage generated by the parametric excitation at $H = 205$ Oe is monitored on a spectrum analyzer (1 kHz resolution bandwidth): an oscillation voltage is detected at $f_p/2 = 1.8$ GHz. (b) The amplitude of this oscillation is measured as the bias field is swept from 195 to 225 Oe. The envelope of the curve should be compared to that in Fig. 2. The maximum parametric signal occurs at $H_{res} = 205$ Oe. The inset shows the threshold behavior ($P_c \simeq +20.7$ dBm) of the power dependence of the spectrum analyzer signal at 1.8 GHz to demonstrate the parametric excitation.

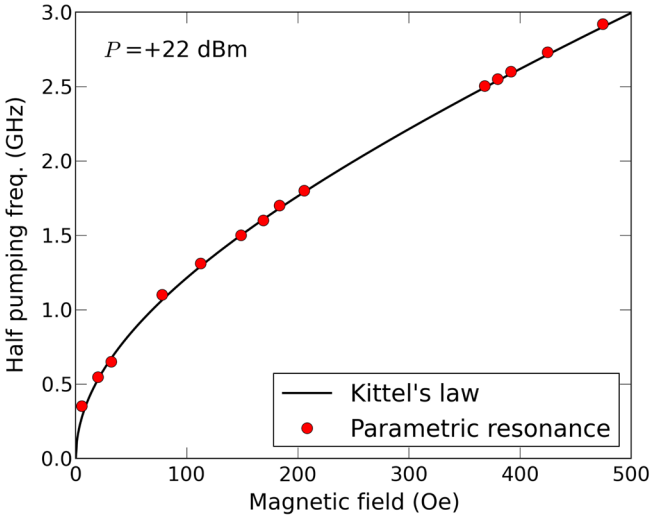

FIG. 5 (color online). Voltage at half the pumping frequency. Red dots correspond to the bias field required to observe the maximum parametric signal detected on the spectrum analyzer at $f_p/2$. The solid line is the Kittel law of the YIG|Pt bilayer [see Fig. 3(a)].

parametric excitation into Pt and converted into a voltage by ISHE. To prove this, we plot in Fig. 4(b) the amplitude of the SA signal measured at $f_p/2$ as a function of H. We find that the amplitude of the signal is maximum at $H =$ 205 G, which is the resonance field determined by standard FMR at 1.8 GHz in Fig. 2 and dies out in a range of about ± 1.5 Oe around this field. We have also checked that this ac voltage signal has a parametric excitation origin by studying its amplitude as a function of the excitation power. One can observe in the inset of Fig. 4(b) that the peak at $f_p/2$ suddenly appears on the SA above a critical power $P_c = +20.7$ dBm, i.e., a critical microwave field $h_c = 0.7$ Oe, in good agreement with the expected threshold for parallel parametric excitation in YIG [24]. We note that the envelope of the parametric excitation signal observed in Fig. 4(b) as a function of H has a shape close to that of the standard FMR peak of Fig. 2. Still, we observe abrupt jumps of the amplitude as H is varied. We find that the details of this variation are very sensitive to changes in the orientation ϕ_H of the bias field. We attribute this to the excitation of spin-wave modes which are almost degenerate with the uniform precession mode [24,28]. We have repeated the same experiment for different excitation frequencies ranging from 0.8 up to 6 GHz. Because the microwave power exceeds the threshold for parallel parametric excitation ($P = +22$ dBm), an ac ISHE voltage at half the excitation frequency is observed on the SA as a function of H when the condition for resonance is met at $f_p/2$ (cf. the Kittel law in Fig. 5). Last, in order to check experimentally that our method eliminates *all* spurious signals, we performed the same series of measurements on a reference sample where the Pt layer was replaced by 15 nm of Al. We found experimentally that *no* electrical signal is produced at $f_p/2$, which allows us to conclude that the layer with strong spin-orbit scattering like Pt is indispensable to observe the ac ISHE voltage.

To gain more insight into the ac ISHE voltage, we would like to comment on its amplitude. For that, we compare the ac and dc components using the $\phi_H = 10°$ configuration [see Fig. 3(b)]. We measure an effective dc voltage $V_{ISHE}(dc) = 1.1\ \mu V$, while in the same conditions, the generated ac voltage is $V_{ISHE}(ac) = 6.2\ \mu V$ (see the Supplemental Material [25]). Thus, we obtain the experimental ratio $[V_{ISHE}(ac)/V_{ISHE}(dc)]_{expt} = 5.6$. We have determined that the angle of precession corresponding to the parametric excitation observed at $H = 20$ Oe is $\theta = 5.1°$. Therefore, one would expect that $[J_s(ac)/J_s(dc)]_{theor} = \xi/\tan\theta = 5.7$, where $\xi = 0.51$ is the ellipticity correction factor for this case (see the Supplemental Material [25]), in excellent agreement with our estimation above.

In conclusion, we have shown that the microwave part of the spin-pumping current emitted by a ferromagnet driven

at resonance can be detected by the inverse spin Hall effect using an adjacent metallic layer with strong spin-orbit scattering [29]. On our millimeter-size YIG|Pt sample, it leads to a microvolt range microwave signal measurable directly on a spectrum analyzer without any preamplification or impedance matching. We believe that this broadband direct detection provides a novel efficient means to study magnetization dynamics in a wide variety of ferromagnetic materials. Further analysis of the measured spectra in the parallel parametric geometry will provide new insights into the spin-wave competition in the nonlinear regime. The phenomenon will also allow dynamical studies of the process of spin transfer at the interface with strong spin-orbit nonmagnetic metals [30–32].

This research was supported by the French ANR Grant Trinidad (ASTRID 2012 Program) and by the RTRA-Triangle de la Physique Grant-2011 Spinoscopy.

*Corresponding author.
oklein@cea.fr

[1] T. Jungwirth, J. Wunderlich, and K. Olejnik, Nat. Mater. **11**, 382 (2012).
[2] S. O. Valenzuela and M. Tinkham, Nature (London) **442**, 176 (2006).
[3] T. Kimura, Y. Otani, T. Sato, S. Takahashi, and S. Maekawa, Phys. Rev. Lett. **98**, 156601 (2007).
[4] Y. Otani and T. Kimura, IEEE Trans. Magn. **44**, 1911 (2008).
[5] M. I. Dyakonov and V. I. Perel, JETP Lett. **13**, 467 (1971).
[6] J. E. Hirsch, Phys. Rev. Lett. **83**, 1834 (1999).
[7] Y. Tserkovnyak, A. Brataas, G. E. W. Bauer, and B. I. Halperin, Rev. Mod. Phys. **77**, 1375 (2005).
[8] G. Woltersdorf, M. Buess, B. Heinrich, and C. H. Back, Phys. Rev. Lett. **95**, 037401 (2005).
[9] B. Heinrich, C. Burrowes, E. Montoya, B. Kardasz, E. Girt, Y.-Y. Song, Y. Sun, and M. Wu, Phys. Rev. Lett. **107**, 066604 (2011).
[10] E. Saitoh, M. Ueda, H. Miyajima, and G. Tatara, Appl. Phys. Lett. **88**, 182509 (2006).
[11] K. Ando, Y. Kajiwara, S. Takahashi, S. Maekawa, K. Takemoto, M. Takatsu, and E. Saitoh, Phys. Rev. B **78**, 014413 (2008).
[12] K. Ando, T. Yoshino, and E. Saitoh, Appl. Phys. Lett. **94**, 152509 (2009).
[13] O. Mosendz, J. E. Pearson, F. Y. Fradin, G. E. W. Bauer, S. D. Bader, and A. Hoffmann, Phys. Rev. Lett. **104**, 046601 (2010).
[14] O. Mosendz, V. Vlaminck, J. E. Pearson, F. Y. Fradin, G. E. W. Bauer, S. D. Bader, and A. Hoffmann, Phys. Rev. B **82**, 214403 (2010).
[15] Y. Kajiwara, K. Harii, S. Takahashi, J. Ohe, K. Uchida, M. Mizuguchi, H. Umezawa, H. Kawai, K. Ando, K. Takanashi, S. Maekawa, and E. Saitoh, Nature (London) **464**, 262 (2010).
[16] Z. Wang, Y. Sun, M. Wu, V. Tiberkevich, and A. Slavin, Phys. Rev. Lett. **107**, 146602 (2011).
[17] C. W. Sandweg, Y. Kajiwara, A. V. Chumak, A. A. Serga, V. I. Vasyuchka, M. B. Jungfleisch, E. Saitoh, and B. Hillebrands, Phys. Rev. Lett. **106**, 216601 (2011).
[18] H. Kurebayashi, O. Dzyapko, V. E. Demidov, D. Fang, A. J. Ferguson, and S. O. Demokritov, Nat. Mater. **10**, 660 (2011).
[19] L. H. Vilela-Leão, C. Salvador, A. Azevedo, and S. M. Rezende, Appl. Phys. Lett. **99**, 102505 (2011).
[20] A. V. Chumak, A. A. Serga, M. B. Jungfleisch, R. Neb, D. A. Bozhko, V. S. Tiberkevich, and B. Hillebrands, Appl. Phys. Lett. **100**, 082405 (2012).
[21] V. Castel, N. Vlietstra, J. Ben Youssef, and B. J. van Wees, Appl. Phys. Lett. **101**, 132414 (2012).
[22] C. Hahn, G. de Loubens, O. Klein, M. Viret, V. V. Naletov, and J. B. Youssef, Phys. Rev. B **87**, 174417 (2013).
[23] H. J. Jiao and G. E. W. Bauer, Phys. Rev. Lett. **110**, 217602 (2013).
[24] M. Sparks, *Ferromagnetic Relaxation Theory* (McGraw-Hill, New York, 1964).
[25] See Supplemental Material at http://link.aps.org/supplemental/10.1103/PhysRevLett.111.217204 for the sample preparation, the experimental methods, and the derivations of equations.
[26] H. Kurebayashi, O. Dzyapko, V. E. Demidov, D. Fang, A. J. Ferguson, and S. O. Demokritov, Appl. Phys. Lett. **99**, 162502 (2011).
[27] K. Ando and E. Saitoh, Phys. Rev. Lett. **109**, 026602 (2012).
[28] V. V. Naletov, G. de Loubens, V. Charbois, O. Klein, V. S. Tiberkevich, and A. N. Slavin, Phys. Rev. B **75**, 140405 (2007).
[29] Recently, we became aware of a parallel effort also reporting the detection of ac ISHE but in NiFe|Pt by D. Wei, M. Obstbaum, C. Back, and G. Woltersdorf, arXiv:1307.2961.
[30] X. Jia, K. Liu, K. Xia, and G. E. W. Bauer, Europhys. Lett. **96**, 17 005 (2011).
[31] L. Liu, C.-F. Pai, Y. Li, H. W. Tseng, D. C. Ralph, and R. A. Buhrman, Science **336**, 555 (2012).
[32] I. M. Miron, K. Garello, G. Gaudin, P.-J. Zermatten, M. V. Costache, S. Auffret, S. Bandiera, B. Rodmacq, A. Schuhl, and P. Gambardella, Nature (London) **476**, 189 (2011).